

Sensitivity experiments with the simulation model of circulation

5.1 Introduction

Results of ocean circulation models vary depending on the dynamics, spatial resolution, numerical scheme, parameterisation of physical processes and the surface forcing parameters. By changing the forcing parameters and the coefficients, a good insight into the dynamics of circulation can be obtained. Before incorporating an ocean circulation model into a coupled climate model, the parameters of the former must be tuned to obtain adequate model climate. The equatorial ocean is directly driven by the windstress, while poleward of about 5°S, the curl of the windstress control the general circulation through sverdrup dynamics. Hence, the choice of the wind stress climatology is very significant for studying the large-scale dynamics of the oceans, especially for the equatorial regions. Different wind stress products yield substantial differences in the flow pattern, transport magnitude and distribution of flow through island passages. Winds derived from numerical models of atmospheric circulation are not very reliable for the equatorial and near equatorial regions because of the breakdown of the assumption of geostrophy in those large-scale models. Actual observed winds through remote sensing technique would give more reliable information on the wind stress field at the equatorial and near equatorial regions. In this chapter, a sensitivity experiment is carried out with the wind field derived from Quikscat scatterometer. The response of the tropical Indian Ocean to NCEP/NCAR reanalysis wind field and Quikscat winds is also presented in this chapter.

5.2 DATA USED

5.2.1 Wind Field

Climatological wind stress derived from the NCEP reanalysis and Quikscat scatterometer wind field were used for the sensitivity experiments. The wind data derived from NCEP reanalysis has a resolution of $2.5^{\circ} \times 2.5^{\circ}$ in longitude and latitude. This wind field has been bilinearly interpolated to the model grid points which has a spatial resolution of $1^{\circ} \times 0.5^{\circ}$ in the longitude and latitude directions respectively.

The use of $2.5^{\circ} \times 2.5^{\circ}$ resolution of the NCEP reanalysis winds, interpolation of the same to model resolution of $1^{\circ} \times 0.5^{\circ}$ and forcing the model with the latter may not capture small scale features of circulation in the equatorial regions. One sensitivity experiment was carried out by forcing the model with the winds derived from Quikscat scatterometer. The sea winds on Quikscat level-3 daily data set consists of grided values of scalar wind speed, meridional and zonal components of wind velocity, wind speed squared and time given in fraction of a day. The data are on a global grid of 1440 pixels in longitude by 720 pixels in latitude (0.25° grid) and also available with a resolution of 0.5° or 1° from 19 July 1999 to present. To force the model, the meridional and zonal components of the Quikscat $0.5^{\circ} \times 0.5^{\circ}$ resolution wind velocity data are interpolated to the model grid of $1^{\circ} \times 0.5^{\circ}$. The Quikscat wind data was earlier used by Senan et al (2003) to force a GCM of Indian Ocean and yielded good results.

5.2.2 Temperature and Salinity Data

The temperature and salinity data required to drive the model were taken from the climatological atlas of Levitus (1994). These data were available at standard oceanographic depths on a 1° longitude \times 1° latitude grid. Because of the non-availability of synoptic data for individual years, seasons and months, the annual, seasonal and monthly means for any parameter are based on a composite of all the available data regardless of

the year of observations. The Levitus monthly mean data are available up to 1500m of water depth. Beyond 1500m depth, its annual mean values have been utilized.

5.2.3 Net Heat Flux

The heat flux components for forcing the model were derived from the NCEP reanalysis data set. This includes the net longwave radiation, net shortwave radiation, sensible heat flux and latent heat flux data sets with a resolution of 2.5°x2.5° in longitude and latitude. The methodology for the computation of heat flux were given in Chapter – II.

5.2.4 Fresh Water Flux

The mass flux is determined by precipitation minus evaporation and is implemented as the salt flux in the simulation model. The precipitation and evaporation data sets were derived from the monthly means of NCEP reanalysis database. The methodology for the computation of fresh water flux is given in Chapter – II.

The freshwater flux from the rivers Ganges and Brahmaputra in to the Bay of Bengal and the river Indus into the Arabian Sea were also included in the simulation model. The freshwater flux is treated as the negative salinity flux in the model.

5.3 Numerical experiment to study the sensitivity of the Indian Ocean circulation to specification of wind stress climatology

The 33 level state-of-art simulation model was forced with windstress climatology derived from Quikscat winds for 10 years to study the 3-D climatological circulation of the Indian Ocean. The results of the 10th year simulation are then compared with the 10th year simulation using NCEP

windstress climatology. The sensitivity of the solution to specification of windstress climatology is discussed in the following sections.

5.4 Results and discussion

5.4.1 Forcing Comparisons

This section compares the two wind forcing datasets and their effect on the OGCM solution. The spatial distribution of monthly mean resultant windstress derived from Quikscat dataset for the month of January, July, April and October are presented in Fig (5.1.a-d). During January northeasterly winds prevail over the Arabian Sea and Bay of Bengal. The magnitude of windstress reaches a maximum of 1 dynes/cm^2 off the coasts of Somalia and western Bay of Bengal. The strength of northeasterly winds is reduced on reaching the equator with calm winds in the doldrums region, and the windstress increases to 1 dynes/cm^2 in the southern Indian Ocean between 15°S and 30°S .

During July, southeasterly winds with magnitude of the order of 1.5 dynes/cm^2 cross the equator from the southern Indian Ocean, change direction on crossing the equator and prevail as strong southwesterly winds over the entire Arabian Sea and Bay of Bengal. Windstress values reaches upto 6 dynes/cm^2 off the coast of Somalia and 4 dynes/cm^2 off Arabia coast. In the Bay of Bengal, winds are relatively weak with a maximum strength of 2 dynes/cm^2 .

During the transition seasons of April and October, strong southeasterly winds prevail over the southern Indian Ocean. Winds are relatively weak in the Arabian Sea and Bay of Bengal. Easterly winds prevail over the equatorial region with maximum strength of 0.6 dynes/cm^2 during April and 1.2 dynes/cm^2 during October.

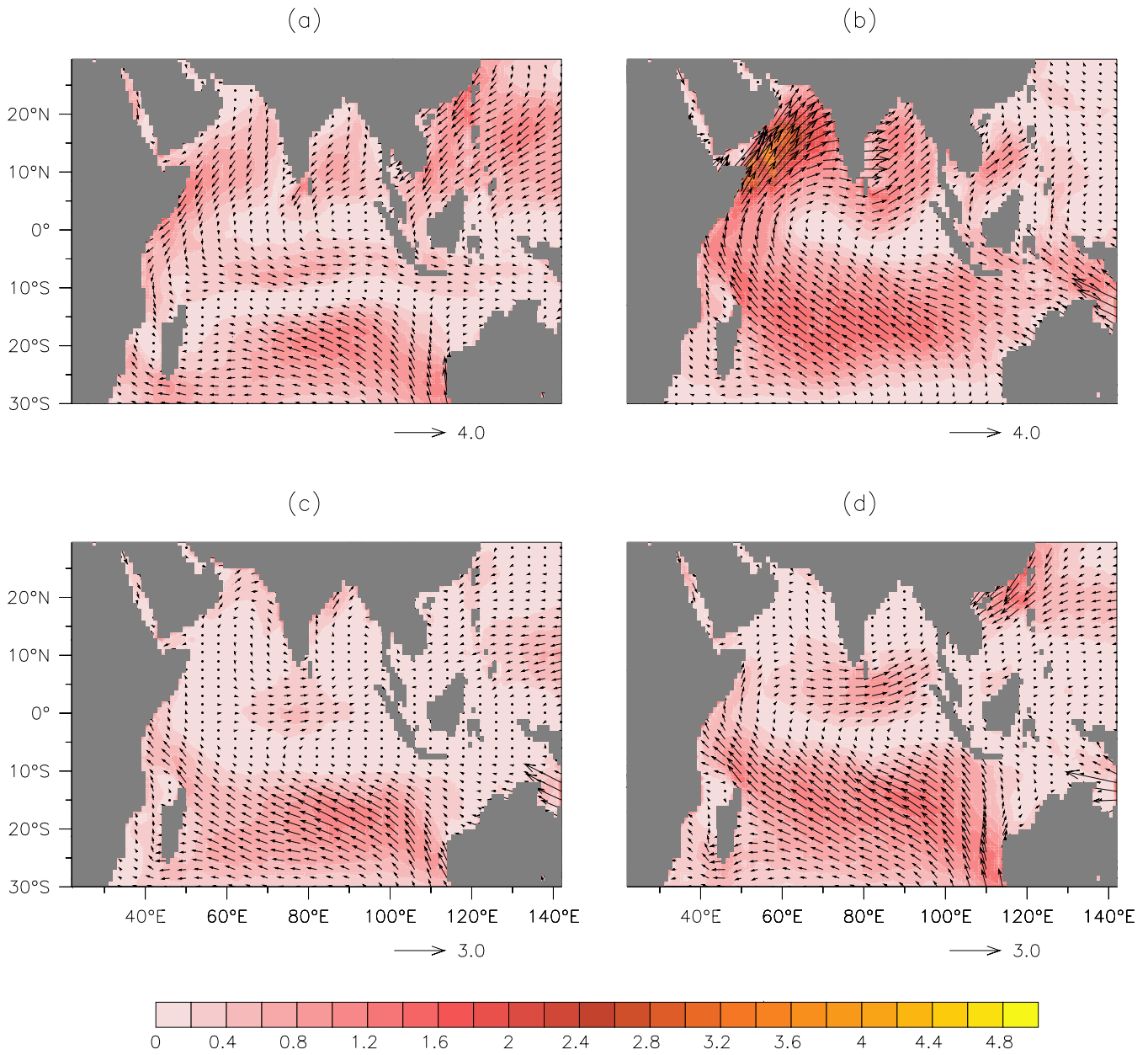


Fig.5.1. Quikscat wind stress fields for different months (dynes/cm²)

(a) January (b) July (c) April (d) October

The difference in zonal and meridional windstress of Quikscat and NCEP (Quikscat-NCEP) for the four months are presented in Figs. 5.2 (a-d) and 5.3 (a-d) respectively. The difference in the zonal component of wind stress is very less ($< 0.2 \text{ dynes/cm}^2$) in the equatorial Indian Ocean for all the four months. The magnitude of the NCEP reanalysis zonal windstress values are lower in the southern Indian Ocean. During July, when strong southwesterly winds prevail over the Arabian Sea, with the core of Findlater Jet centered near the western sector, the NCEP zonal windstress values are higher than Quikscat values by about of 0.6 dynes/cm^2 . These strong zonal windstress values are significant for upwelling processes that takes place off the coasts of Somalia and Arabia during the southwest monsoon season. The difference in the meridional windstress between the two wind products is very less except for the month of July. In July along the west coast of Arabian Sea and off the coast of Somalia and Arabia, the meridional wind stress component of NCEP is higher than Quikscat wind data.

5.4.2 Dynamic response of the model to the wind forcing

5.4.2.1 Barotropic Stream Function

The vertically integrated mass transport stream function for January, July, April and October is presented in Fig. 5.4 (a-d). Maximum transport is observed in the South Equatorial Current region in the southern Indian Ocean with magnitude ranging from 20 Sv to 30 Sv. This is consistent with the Lutjeharms (1997) transport diagram for the southern Indian Ocean, which yielded an SEC transport of 25 Sv upto northern end of Madagascar. During January, the cross equatorial Somali Current transport was found to be 15 Sv and this transport increased to 25 Sv during the southwest monsoon season. During the transition season, when strong eastward currents exist in the equatorial Indian Ocean, the central equatorial Indian Ocean transport was found to be 10 Sv and 15 Sv for April and October respectively.

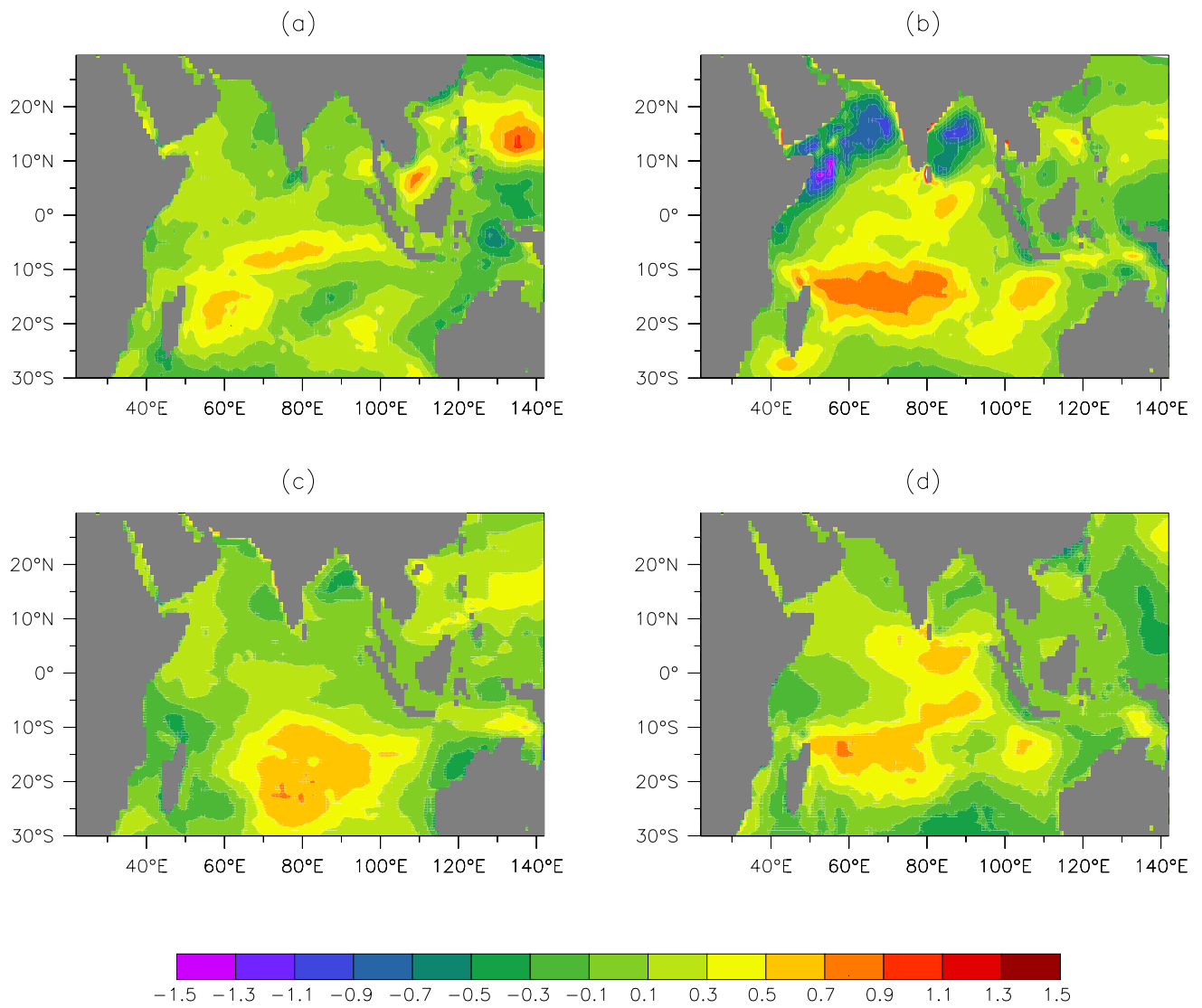


Fig.5.2. Difference in zonal wind stress (Quikscat minus NCEP) in dynes/cm²
 (a) January (b) July (c) April (d) October

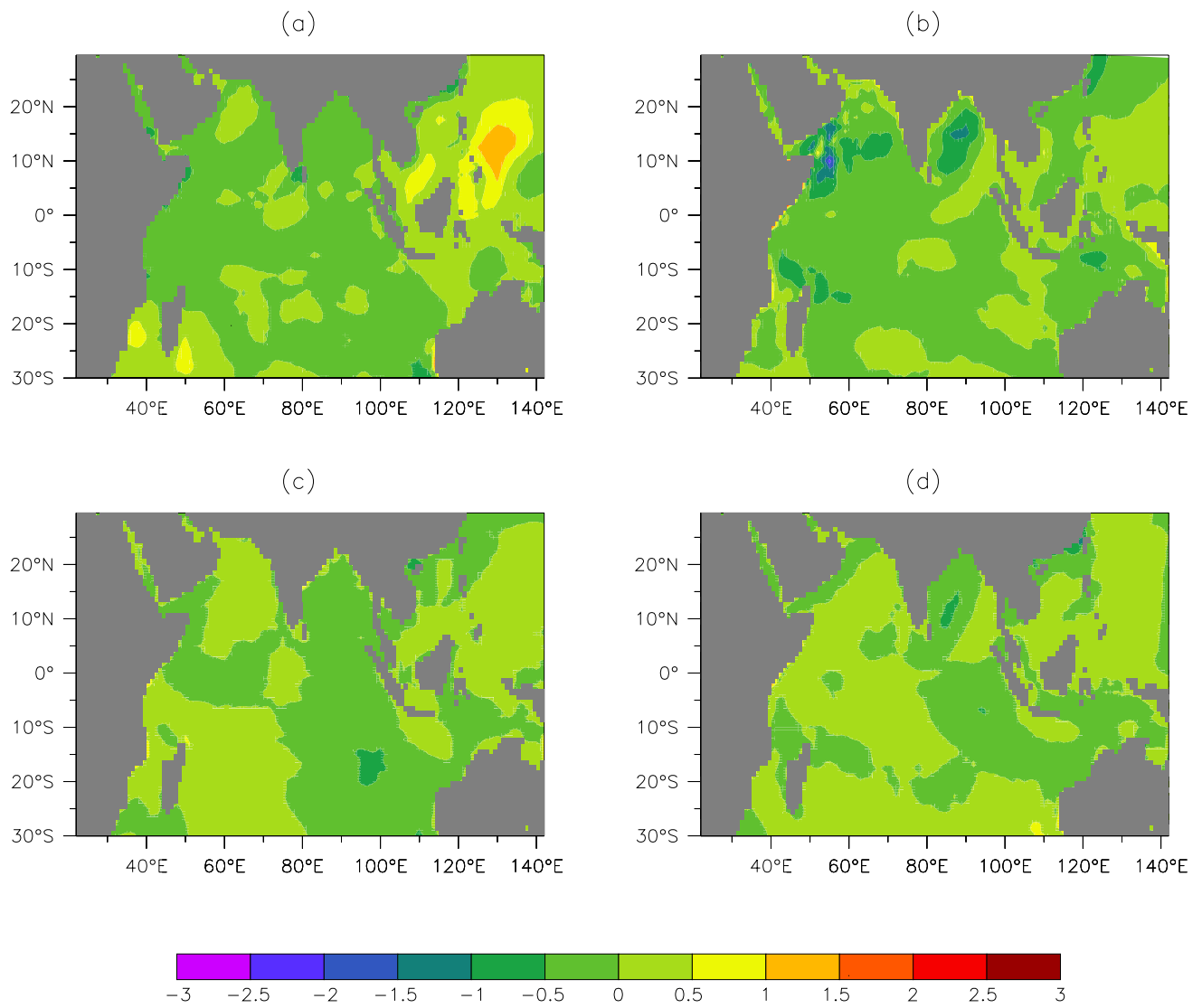


Fig.5.3. Difference in meridional wind stress (Quikscat minus NCEP) in dynes/cm²
 (a) January (b) July (c) April (d) October

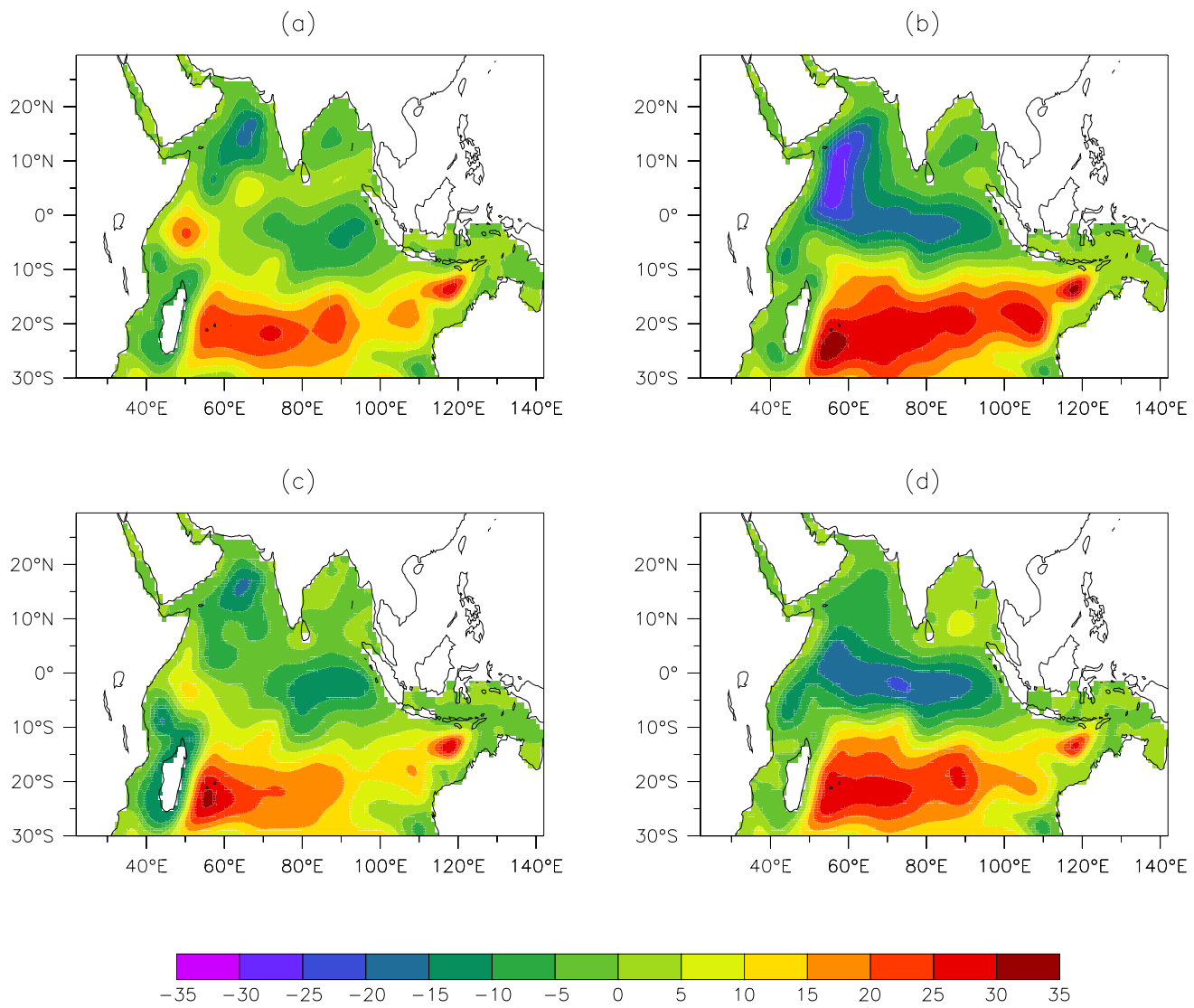


Fig.5.4. Monthly mean mass transport stream function for different months using Quikscat wind forcing
 (a) January (b) July (c) April (d) October

The mass transport stream function (ψ_{OGCM}) of from the NCEP forcing is shown in Fig. 5.5 (a-d). The gyre pattern and the transport magnitude depends mainly on the wind forcing of the model. The largest difference in ψ_{OGCM} occur in the equatorial regions where large difference in the windstress is observed. During April and October, this difference is higher when strong eastward equatorial currents prevail over the equatorial Indian Ocean.

5.4.2.2 Spatial Variability of Currents at the Surface

(i) Surface velocity fields for January

The surface velocity vectors forced by Quikscat winds and the difference in current fields due to Quikscat and NCEP wind forcings for the month of January is presented in Fig. 5.6. The permanent current systems observed in the Indian Ocean during January are the SEC, EACC, SECC in the southern Indian Ocean, the cross equatorial Somali Current, NEMC, and the WICC in the Arabian Sea and EICC in the Bay of Bengal. Driven by the southeast trades of the southern hemisphere, the SEC appears to be more zonal flowing westward with a magnitude of 20cm/s between latitudes 10°S and 22°S. At 17°S, the SEC splits into a strong northward flow called the North East Madagascar Current (NEMC) and a relatively weak southward flow called the South East Madagascar Current (SEMC). The northward flowing NEMC feeds in to the EACC that flows northward with a magnitude of 20cm/s. The Somali Current flows southward across the equator with a maximum strength of 90cm/s. The SC encounters the EACC at 2-5°S causing a confluence and eastward flow which supplies the SECC with a magnitude of 40cm/s. In the Arabian Sea, the WICC has a magnitude of 20cm/s flowing poleward against the prevailing wind direction. The NMC exists between the equator and 4°N with a magnitude of 40cm/s.

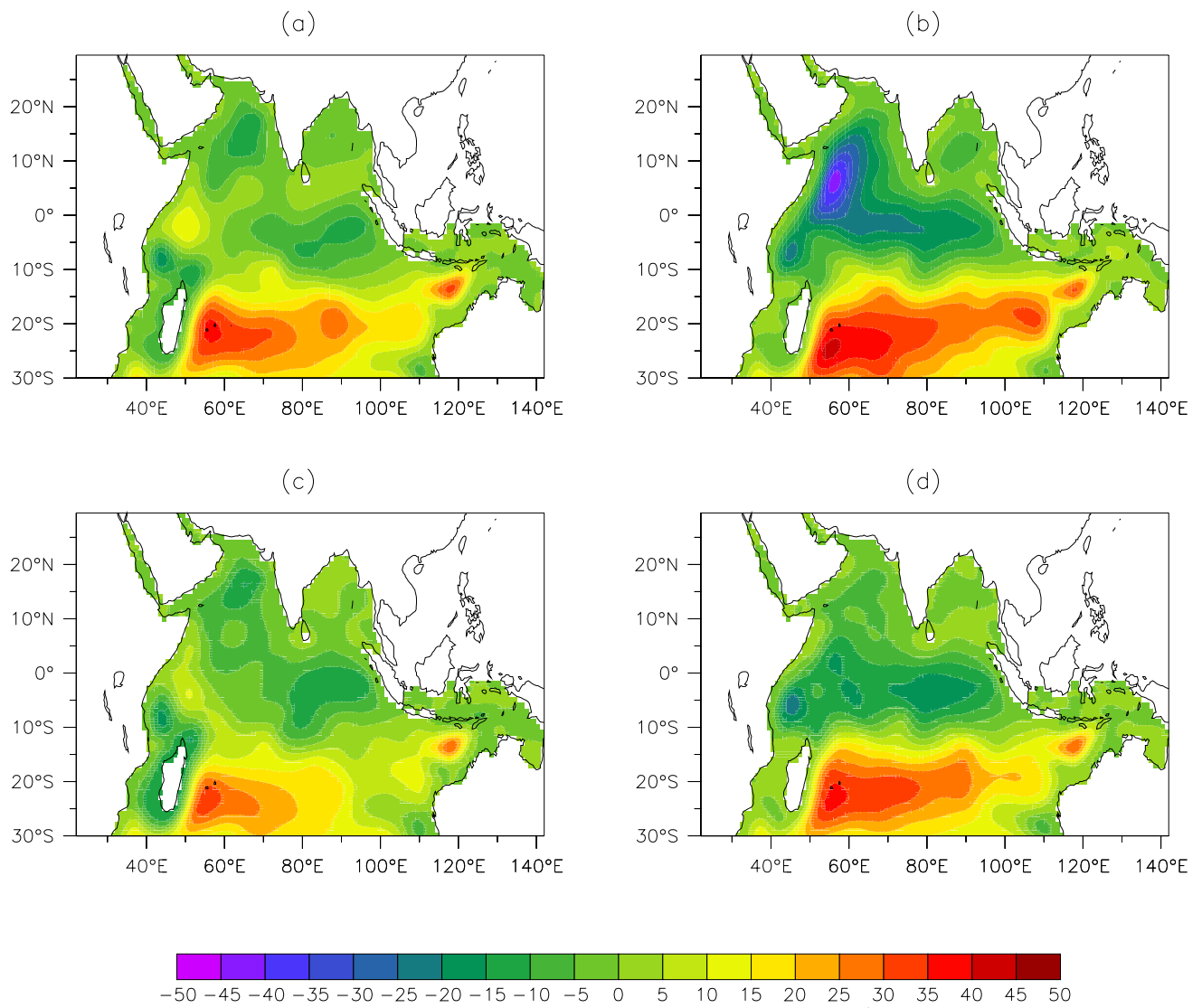


Fig.5.5. Monthly mean mass transport stream function for different months using NCEP wind forcing
 (a) January (b) July (c) April (d) October

The circulation in the Bay of Bengal is dominated by the presence of an anticyclonic gyre during February-May with a poleward EICC forming the western boundary current. The EICC with a magnitude of nearly 10cm/s is relatively weak during January.

The difference in surface velocity fields for January due to NCEP and Quikscat wind forcings is presented in Fig. 5.6. Between 5°N and the equator, which is the region of the Northeast Monsoon Current (NMC), surface velocity fields are 5 to 10cm/s stronger for NCEP forcing than Quikscat forcing. The zonal and meridional components of wind stress in this region do not show any difference in two wind datasets in this region. In the central equatorial Indian Ocean, model velocity fields driven by Quikscat forcing are higher by 5cm/s as compared to NCEP wind driven velocity fields. This is mainly due to the presence of higher zonal component of wind stress values in this region.

(ii) Surface velocity fields for July

The surface velocity vectors for July forced by Quikscat winds and the difference in current fields due to Quikscat and NCEP is presented in Fig. 5.7. During the southwest monsoon season (July), the SEC extends up to 22°S with a magnitude of 20cm/s. The SEC then feeds into EACC and EACC supplies the northward flowing Somali Current. Forced by the strong southwesterly winds of the southwest monsoon season, the SC attains a maximum speed of 150cm/s and crosses the equator at 4°N and there it turns offshore with a cold upwelling core at its left side. A part of SC circulates around the equator forming the Southern Gyre (SG) and another turns offshore at 8°N forming the Great Whirl (GW). Both these circulation features are well reproduced in the model simulation. The SC feeds the eastward flowing Southwest Monsoon Current (SMC).

In the Bay of Bengal, the anticyclonic gyre breaks up with the onset of the southwest monsoon season. The circulation consists of southward flow in

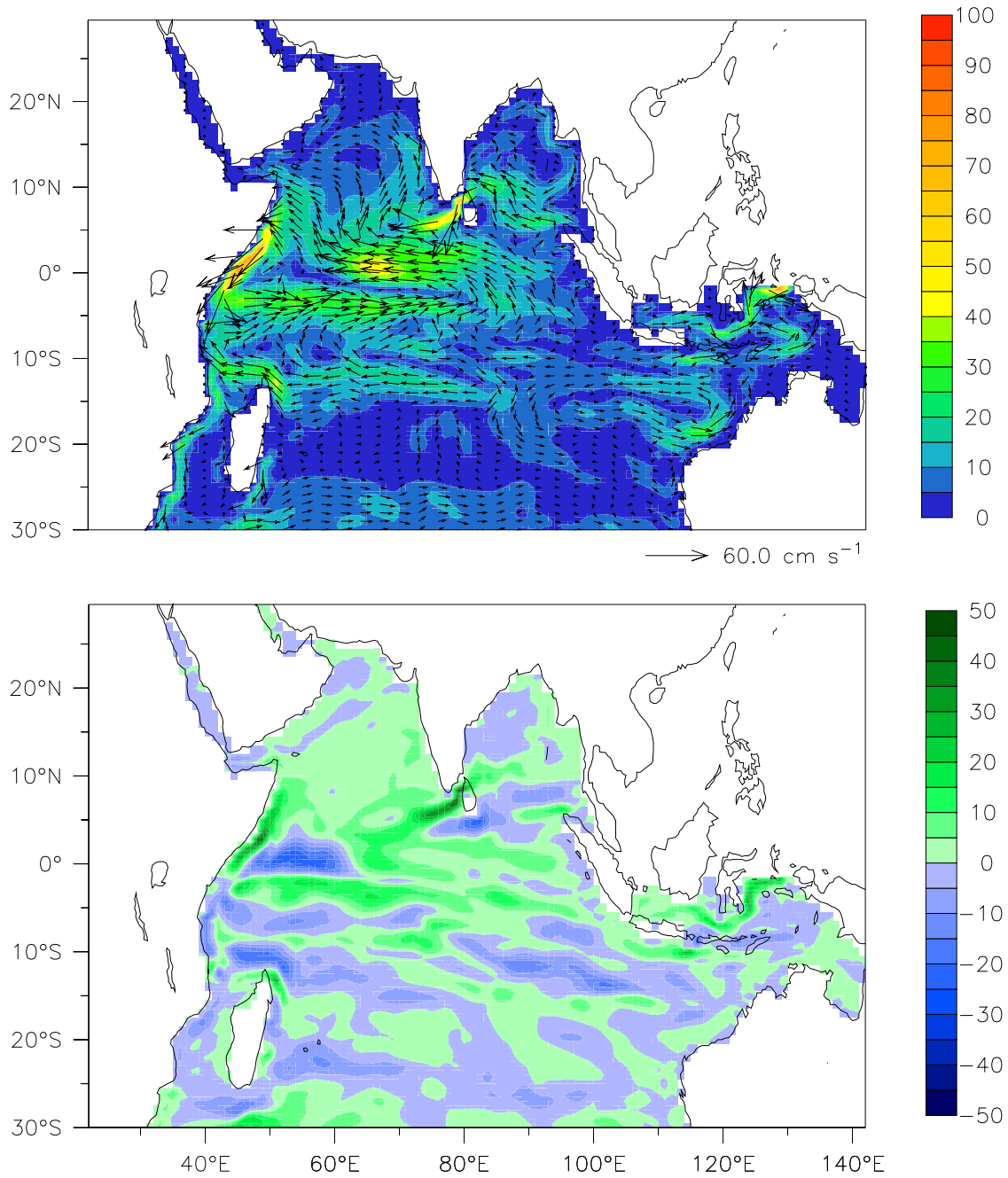


Fig.5.6. Surface velocity fields (cm/s) forced by Quikscat winds (top panel) and difference in surface velocity fields due to Quikscat and NCEP wind forcing for January (lower panel)

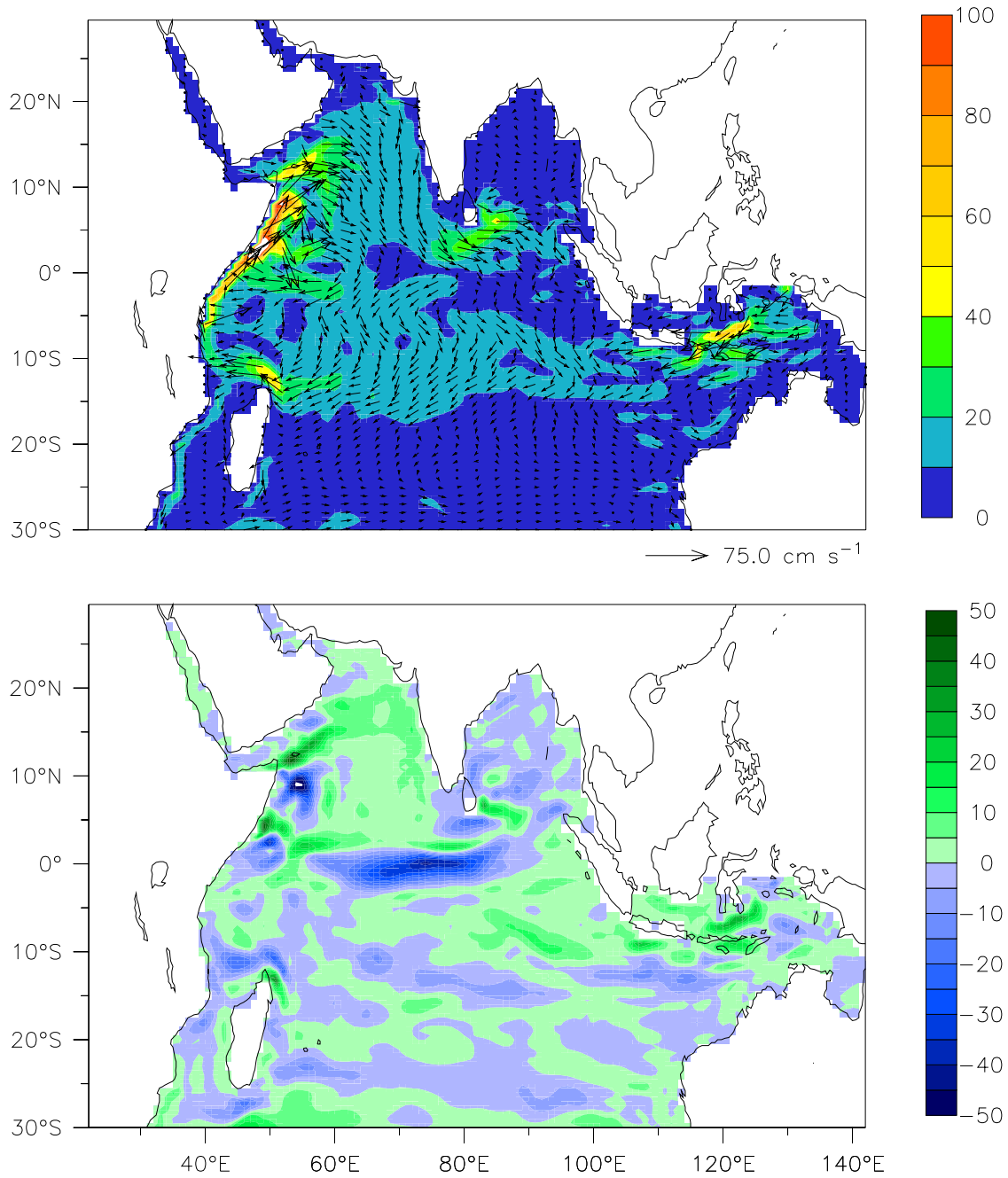


Fig.5.7. Surface velocity fields (cm/s) forced by Quikscat winds (top panel) and difference in surface velocity fields due to Quikscat and NCEP wind forcing for July (lower panel)

the northern and southern part of the Bay of Bengal contributing to the East India Coastal Current (EICC). Though the winds are strong during the monsoon season, the circulation in the Bay of Bengal is best developed during the transition seasons.

In the Somali Current region during July, the surface velocity fields are higher by 20-30cm/s for NCEP forcing than for the Quikscat forcing. The NCEP wind winds are stronger than Quikscat winds contributing to higher current values for NCEP forcing in the Somali region. In the central equatorial Indian Ocean, the Southwest Monsoon Current (SMC) is 30 cm/s stronger in NCEP forcing. The modeling studies of McCreary et al., (1993) and Vinayachandran et al., (1999) contributed two driving mechanisms for SMC, one is by remote forcing and the other by local forcing by wind stress curl which is strongest in the southwestern Bay of Bengal. In the southwestern Bay of Bengal, the NCEP wind stress are stronger than Quikscat winds and this difference in the wind stress forcing generates stronger eastward current.

(iii) Surface Velocity Fields for April and October

The surface velocity vectors forced by Quikscat winds and the difference in current fields due to Quikscat and NCEP wind forcing for the month of April and October are presented in Figs. 5.8 and 5.9 respectively. During April and October, the main feature of circulation observed in the Indian Ocean are the strong eastward Equatorial Jets (EJ) forced by the strong eastward semiannual component of windstress over the equatorial Indian Ocean. In the computed results EJ's were reproduced with a maximum strength of 80cm/s and 70cm/s during April and October respectively. These stronger eastward EJ's derive their existence from the more realistic strong eastward winds derived from the Quikscat wind climatology.

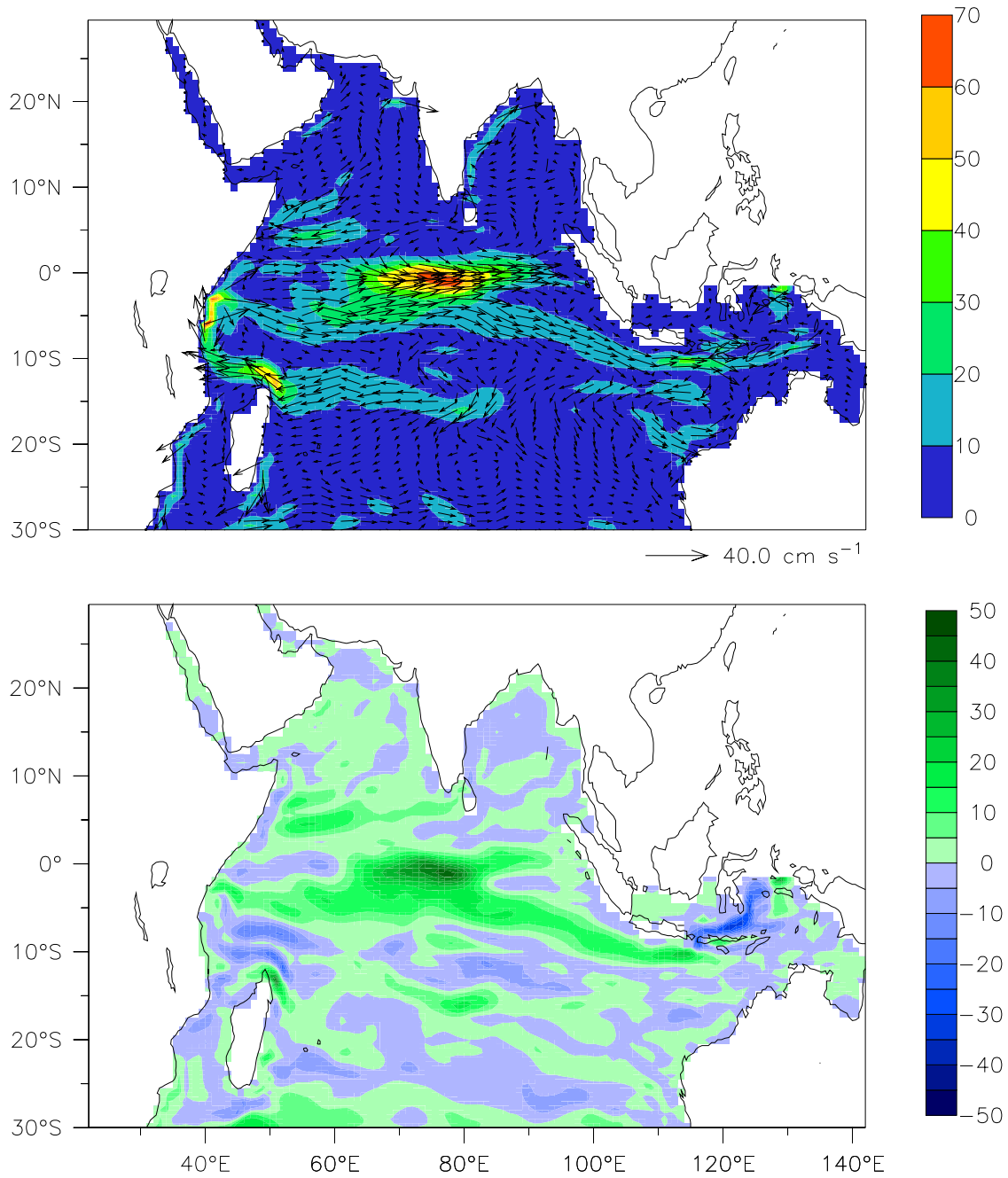


Fig.5.8. Surface velocity fields (cm/s) forced by Quikscat winds (top panel) and difference in surface velocity fields due to Quikscat and NCEP wind forcing for April (lower panel)

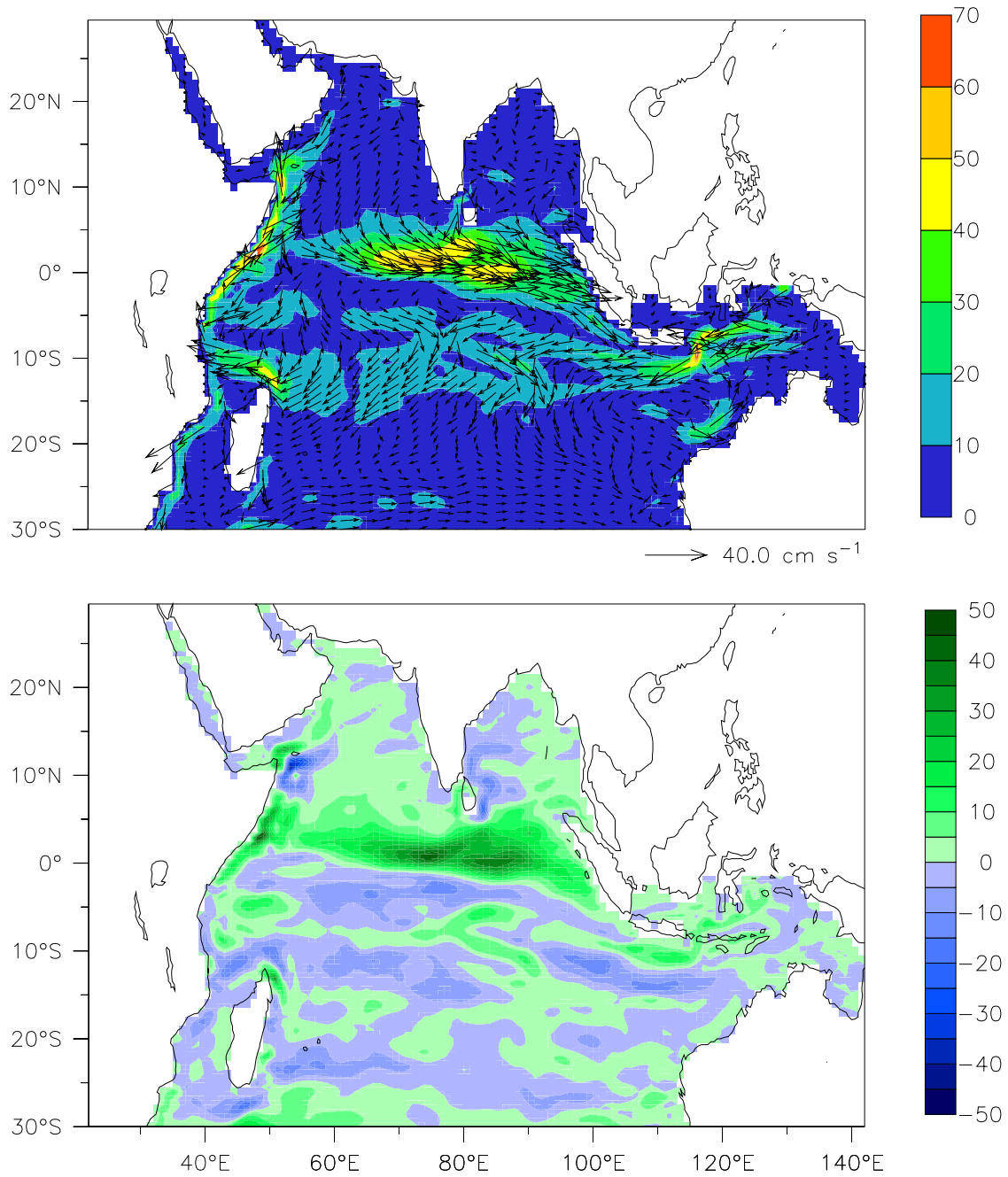


Fig.5.9. Surface velocity fields (cm/s) forced by Quikscat winds (top panel) and difference in surface velocity fields due to Quikscat and NCEP wind forcing for October (lower panel)

Many observational and modeling studies attributed direct forcing by the semi-annual component of the winds as the dominant forcing mechanism for the EJ's. This sensitivity experiment is particularly important for the study of EJ's as the two wind datasets (Quikscat and NCEP) shows much difference in the equatorial region. Quikscat data being derived from the insitu observations, it is more realistic in the equatorial region. During April and October, the Quikscat wind speeds are higher than NCEP values over the equatorial Indian Ocean. This yields stronger EJ's in the Quikscat solutions of the model. During April and October, the EJ's were 25cm/s stronger in Quikscat forcing than NCEP.

5.5 Conclusions

A state of art simulation model with 33 levels in the vertical has been used to investigate the sensitivity of a primitive equation sigma co-ordinate model of Indian Ocean to difference in windstress climatology. Numerical experiment was conducted by forcing the model with monthly mean climatological windstress derived from Quikscat dataset. The results of the simulations were compared with the results of the model driven with NCEP reanalysis wind stress climatology. Large zonal windstress difference was observed between the two wind data sets over the equatorial Indian Ocean. The NCEP winds being model simulated may not be accurate in the equatorial regions as compared to in situ Quikscat winds. The monthly mean response of the model to two wind datasets were compared for the mass transport stream function and surface velocities for the months January, July, April and October representing the four seasons. The model driven with Quikscat winds reproduced equatorial circulation features more realistically than the NCEP forcing. The current systems were intensified in the equatorial Indian Ocean when the model was driven with the Quikscat wind forcing. The equatorial Jets of the Indian Ocean were strengthened by about 20cm/s during April and October. It is has been observed that the simulation model response to

Quikscat winds is dynamically consistent with the difference in the mean surface wind fields. The sensitivity experiment reveals that the surface circulation is mainly controlled by windstress forcing and hence the thermodynamic forcing play minor role at the upper levels.